Chinese Journal of Chemical Engineering 53 (2023) 317–323

Contents lists available at ScienceDirect

Chinese Journal of Chemical Engineering

journal homepage: www.elsevier.com/locate/CJChE

Full Length Article

Kinetics of the direct reaction between ozone and phenol by high-gravity intensified heterogeneous catalytic ozonation

Kechang Gao, Shengjuan Shao, Zhixing Li, Jiaxin Jing, Weizhou Jiao *, Youzhi Liu

Shanxi Province Key Laboratory of Higee-Oriented Chemical Engineering, North University of China, Taiyuan 030051, China

ARTICLE INFO

Article history:
Received 6 September 2021
Received in revised form 22 January 2022
Accepted 24 January 2022
Available online 14 February 2022

Keywords:
High-gravity technique
Heterogeneous catalysis
Ozone
Phenol
Kinetics of the direct reaction

ABSTRACT

In this study, high-gravity intensified heterogeneous catalytic ozonation is utilized for treatment of phenol-containing wastewater, and the kinetics of the direct reaction between ozone and phenol in the presence of excess tertiary butanol (TBA) is investigated. It is revealed that the direct reaction between ozone and phenol in the rotating packed bed (RPB) follows the pseudo-first-order kinetics with a reaction rate constant higher than that in the conventional bubbling reactor (BR). Under different conditions of temperature, initial pH, high-gravity factor, and gaseous ozone concentration, the apparent reaction rate constant varies in the range of 0.0160–0.115 min^{-1}. An empirical power-exponential model is established to characterize the effects of these parameters on the direct reaction between ozone and phenol by high-gravity intensified heterogeneous catalytic ozonation.

1. Introduction

Phenol is often present in large quantities in wastewater discharged from coal processing, dyeing and coking industries [1–3], and it has high teratogenic, carcinogenic and mutagenic potential that may lead to serious consequences to humans even in a trace amount [4]. Because of this, phenol is regarded as a priority pollutant by the US EPA (United States Environmental Protection Agency) [5], and a great deal of effort has been made in the treatment of phenol wastewater. Ozone (O_3) is a strong oxidant with a redox potential of 2.07 V and ozonation would cause no secondary pollution as only oxygen is produced from the reaction of O_3 with organic pollutants. These desired properties make O_3 an attractive candidate for treatment of organic wastewater [6,7]. However, given the low solubility of O_3 in water and the low selectivity of organic compounds, incomplete reaction is likely to occur between O_3 and organic pollutants and thus limits the practical application of ozonation.

Heterogeneous catalytic ozonation has emerged as an effective and environmentally friendly method for the treatment of organic wastewater [8], in which solid catalysts are used in order to overcome the problems, such as difficult separation of catalysts and secondary pollution, that are likely to occur in homogeneous catalytic ozonation. Supported transition metal oxides, such as Cu-MnO_X/γ-Al_2O_3 [9] and Cu-Ni-Co/γ-Al_2O_3 [10], have been widely used in heterogeneous catalytic ozonation due to their low preparation cost and high catalytic activity. O_3 can be adsorbed on the active sites on the catalyst surface and then decomposed into hydroxyl radicals *via* a series of chain reactions, and these hydroxyl radicals have high oxidative capacity and react non-selectively with organic pollutants. As a result, the organic pollutants in wastewater can be completely mineralized into CO_2 and H_2O [11]. Wu *et al.* [12] prepared mesoporous Mn-CeO_X/γ-Al_2O_3 for catalytic ozonation of bromaminic acid (BAA) in an aeration device, and the results revealed that Mn-CeO_X/γ-Al_2O_3 significantly improved the degradation of BAA, but the mineralization rate was not as high as expected because the low mass transfer rate of O_3 from the gas phase to the liquid phase led to the dissolution of less O_3 and subsequently the formation of less ·OH. Thus, there is a need to increase the mass transfer rate of gas-phase O_3 in order to improve the degradation efficiency of organic pollutants [13,14].

The high-gravity technique is known as a novel chemical process intensification technique [15], whereby a high-gravity field is created by the high-speed rotating packing, so that the liquid flowing in the porous media or pores can be sheared into small droplets or thin films. Thus, the mass transfer rate is increased as a result of the large specific surface area and fast renewal of the interface [16,17]. Jiao *et al.* [18] found that the mass transfer coefficient in the O_3-deionized water adsorption process in rotating packed bed (RPB) was 5.6 times that in an aeration reactor under the same experimental conditions. Thus, it is concluded that the

* Corresponding author. Fax: 86 351 3921497.
E-mail address: zbdxjwz@nuc.edu.cn (W. Jiao).

https://doi.org/10.1016/j.cjche.2022.01.021
1004-9541/

high-gravity technique has the potential to enhance the mass transfer of O_3 and thus the amount of O_3 dissolved in water in unit time.

High-gravity intensified heterogeneous catalytic ozonation could be a method of choice for treatment of organic wastewater. Wei *et al.* [19] found that under the optimal conditions, the removal rate of phenol by heterogeneous catalytic ozonation with Fe-Cu-MnO_X/γ-Al_2O_3 catalysts in RPB reached 100% after 7 min and the removal rate of total organic carbon (TOC) reached 96.42% after 30 min. It should be noted that the mineralization rate in RPB was about 21% higher than that in a bubbling reactor. The high-gravity technique can improve not only the mass transfer of O_3 but also the turbulence of the liquid [20–22]. However, despite a large number of studies on the optimization of degradation process parameters, little is known about the reaction kinetics for the heterogeneous catalytic ozonation of phenol in RPB. Obviously, such knowledge is essential to better understand the degradation mechanism of organic pollutants by catalytic ozonation in a high-gravity environment and to improve the design of RPB. It should be noted that the degradation of organic pollutants is the result of the direct reaction with O_3 and the indirect reaction with free radicals such as ·OH generated from the decomposition of O_3 [23]. O_3 can attack electron-rich centers *via* direct electrophilic reactions, and then the aromatic ring is opened to form biodegradable low-molecular weight compounds [24]. Thus, it is important to understand the direct reaction between O_3 and phenol in a high-gravity environment.

In this study, the free radical scavenger tertiary butanol (TBA) is added to the simulated phenol wastewater to investigate the kinetics of the direct reaction between O_3 and phenol in high-gravity intensified heterogeneous catalysis using the solute consumption method [23]. The effects of initial solution pH, high-gravity factor, gas-phase O_3 concentration, and temperature on the reaction rate are investigated using the single-factor variable method, and an empirical kinetic model is established to describe the effects of these parameters on the reaction rate.

2. Experimental

2.1. Materials and instruments

Spherical Fe-Mn-CuO_X/γ-Al_2O_3 particles (diameter: 3–5 mm; specific surface area: 212.94 $m^2 \cdot g^{-1}$; pore volume: 0.705 $cm^3 \cdot g^{-1}$; pore size: 5.61 nm) were used as the catalyst. The reagents used in the experiment included phenol (PhOH), tertiary butanol (TBA), sodium hydroxide (NaOH), sulfuric acid (H_2SO_4) and sodium thiosulfate ($Na_2S_2O_3$), all of which were analytically pure. All solutions were prepared with deionized water. The instruments used in this study included a RPB (Research Centre of Shanxi Province for High Gravity Chemical Engineering and Technology, China, Table 1); an ozone generator (CF-G-3-20g, Shandong Qingdao Guolin Technology Co., Ltd., China); a Dionex Ultimate 3000 instrument (USA) for high-performance liquid chromatography; a pH detector (FE28-Standard, Swiss MT Group); a gas-phase ozone concentration detector (3S-J5000; Beijing Tonglin Technology Co., Ltd., China); and a liquid-phase ozone concentration detector (DOZ5500; Beijing Tonglin Technology Co., Ltd., China).

Table 1
The equipment parameters of the RPB

Parameters	Values
Inner diameter/mm	90
Outer diameter/mm	30
Packing height/mm	60
Packing porosity/$m^3 \cdot m^{-3}$	0.68

2.2. Analytical methods

2.2.1. The degradation efficiency of PhOH

The PhOH concentration was determined by high-performance liquid chromatography (HPLC; Dionex Ultimate 3000, USA) using a C18 reversed phase column, where the detection wavelength was set at 270 nm, the methanol (chromatographic grade; Kemiou Chemical Reagent C.o. Ltd., China)-water mixture (60:40) acted as the mobile phase with a flow rate of 1.0 $ml \cdot min^{-1}$, the column temperature was set to 298 K, and the injection volume was set to 20 μl.

The degradation efficiency of PhOH is defined as follows:

$$\eta_{\mathrm{PhOH}} = \left[(C_0 - C_t)/C_0\right] \times 100\% \tag{1}$$

where η (%) is the degradative efficiency of PhOH, C_0 is the initial PhOH concentration in the solution ($mg \cdot L^{-1}$), and C_t is the PhOH concentration after reaction ($mg \cdot L^{-1}$).

2.2.2. The rate constant of the direct reaction between O_3 and phenol

In the high-gravity intensified heterogeneous catalytic ozonation of phenol, phenol can react directly with O_3 dissolved in water and indirectly with ·OH generated from the self-decomposition or Fe-Mn-CuO_X/γ-Al_2O_3 catalyzed decomposition of dissolved O_3. The reaction rate can be described as follows:

$$-\frac{\mathrm{d}C_{\mathrm{PhOH}}}{\mathrm{d}t} = k_{\mathrm{O_3,PhOH}} C_{\mathrm{O_3},t} C_{\mathrm{PhOH},t} + k_{\cdot\mathrm{OH,PhOH}} C_{\cdot\mathrm{OH},t} C_{\mathrm{PhOH},t} \tag{2}$$

where $k_{\mathrm{O_3,PhOH}}$ is the rate constant of the direct reaction between O_3 and phenol, $L \cdot mol^{-1} \cdot s^{-1}$; $C_{\mathrm{O_3},t}$, $C_{\mathrm{PhOH},t}$ and $C_{\cdot\mathrm{OH},t}$ are the concentrations of dissolved O_3, phenol and ·OH at time t, $mol \cdot L^{-1}$, respectively; and $k_{\cdot\mathrm{OH,PhOH}}$ is the rate constant of the indirect reaction between phenol and ·OH, $L \cdot mol^{-1} \cdot s^{-1}$.

In order to elucidate the direct reaction kinetics, excess TBA was added to scavenge ·OH. In this case, the reaction rate for the direct reaction between O_3 and phenol can be described as follows:

$$-\frac{\mathrm{d}C_{\mathrm{PhOH}}}{\mathrm{d}t} = k_{\mathrm{O_3,PhOH}} C_{\mathrm{O_3},t} C_{\mathrm{PhOH},t} \tag{3}$$

where $k_{\mathrm{O_3,PhOH}}$ is the rate constant of the direct reaction, $L \cdot mol^{-1} \cdot s^{-1}$.

Note that $k_{\mathrm{O_3,PhOH}}$ could not be determined directly from Eq. (3), and instead it is determined by the solute consumption method in this study. For this purpose, excess O_3 is provided to ensure a constant O_3 concentration throughout the experiment. In this case, the reaction between O_3 and phenol is assumed to follow the pseudo-first-order kinetics, and thus Eq. (3) can be changed into:

$$-\frac{\mathrm{d}C_{\mathrm{PhOH}}}{\mathrm{d}t} = k_{\mathrm{app}} C_{\mathrm{PhOH},t} \tag{4}$$

$$k_{\mathrm{app}} = k_{\mathrm{O_3,PhOH}} C_{\mathrm{O_3},t} \tag{5}$$

where k_{app} is the apparent rate constant of the direct reaction between O_3 and phenol, s^{-1}.

Eq. (4) can be simplified into:

$$\ln(C_{\mathrm{PhOH},0}/C_{\mathrm{PhOH},t}) = k_{\mathrm{app}} t \tag{6}$$

It is known from Eq. (4) that once the phenol concentration at t is known, the apparent rate constant of the direct reaction between O_3 and phenol can be calculated.

2.3. Reaction kinetics

The reaction kinetics is used to describe the reaction rate as a function of time under the effects of different factors. It is known that the degradation rate of phenol is closely associated with temperature, initial solution pH, high-gravity factor and gas-phase O_3 concentration, and their effects can be described by the following empirical power-exponential model [25,26]:

$$C_{PhOH,t} = C_{PhOH,0}\exp(-k_{O_3,PhOH}t) \quad (7)$$

$$k_{O_3,PhOH} = A\exp(-E_a/RT)C_{OH^-}^{m}C_{O_3}^{n}N^{p} \quad (8)$$

Taking the logarithm on both sides yields:

$$\ln k_{O_3,PhOH} = \ln A - \frac{E_a}{RT} + m\ln C_{OH^-} + n\ln C_{O_3} + p\ln N \quad (9)$$

where $k_{O_3,PhOH}$ is the apparent rate constant of the direct reaction between O_3 and phenol, min^{-1}; A is the pre-exponential factor; E_a is the apparent activation energy of the direct reaction, $J{\cdot}mol^{-1}$; R is the gas constant, 8.314 $J{\cdot}mol^{-1}{\cdot}K^{-1}$; T is the reaction temperature, K; C_{OH^-} is the OH^- concentration, $mol{\cdot}L^{-1}$; C_{O_3} is the gas-phase O_3 concentration, $mg{\cdot}L^{-1}$; N is the rotation speed of the rotor, $r{\cdot}min^{-1}$; and m, n and p are the reaction orders.

2.4. Catalytic ozonation experiments

The experimental setup for catalytic ozonation is schematically shown in Fig. 1.

A mixture of O_3 and O_2 was produced from O_2 stored in the oxygen cylinder using an O_3 generator, and the O_3 concentration was measured using a gas-phase O_3 concentration detector. The mixture was introduced into RPB from the gas inlet and flowed through the packing along the axis. The phenol solution was pumped from the storage tank into RPB using a circulating pump, and then sheared into micro-elements by the high-speed rotating packing in order to fully react with the gas mixture passing through the packing. In the liquid pipeline, the liquid-phase O_3 concentration was measured using a liquid-phase O_3 concentration detector. Samples were taken at a regular time interval, and 0.01 $mg{\cdot}L^{-1}$ $Na_2S_2O_3$ solution was added dropwise immediately to terminate the reaction of O_3 in the liquid. The exhaust gas was discharged from the air outlet and absorbed by KI solution. The same experiments were also performed in a bubbling reactor (BR) under the same conditions for comparison.

3. Results and Discussion

In this study, TBA is used to scavenge ·OH in order to investigate the direct reaction between O_3 and phenol. As the reaction rate constant of TBA with ·OH (4.6×10^8 $L{\cdot}mol^{-1}{\cdot}s^{-1}$) is 11 orders of magnitude higher than that with O_3 (0.003 $L{\cdot}mol^{-1}{\cdot}s^{-1}$), ·OH can be completely scavenged in the presence of excess TBA [27,28]. Fig. 2 reveals that the removal rate of phenol in the presence of 10 ml of TBA (87.9%) is 10% lower than that in the absence of TBA. This is because in the former case phenol can react with only dissolved O_3 due to scavenging of ·OH by TBA; while in the absence of TBA, phenol can react directly with dissolved O_3 and indirectly with ·OH generated from the self-decomposition or Fe-Mn-CuO_X/γ-Al_2O_3 catalyzed decomposition of dissolved O_3 [29]. However, as the amount of ·OH generated is much lower than that of O_3, the addition of excess TBA leads to no further decrease in the removal rate of phenol. In this study, the indirect reaction between phenol and ·OH can be completely inhibited at a TBA dosage of 10 ml, leaving only the direct reaction between O_3 and phenol [30]. Thus, the TBA dosage is set to 10 ml in the following experiments.

Fig. 3 shows the rate constant of the direct reaction between O_3 and phenol in RPB and BR. It is seen that under the same conditions, the rate constant is 0.0421 min^{-1} in RPB and 0.0246 min^{-1} in BR, indicating that RPB can facilitate the direct reaction between O_3 and phenol. This is because the liquid can be sheared into microelements by the high-speed rotating packing, which can increase the gas–liquid contact area [15] in unit time and thus increase the reaction rate between O_3 and phenol.

3.1. The kinetics of the direct reaction between O_3 and phenol in RPB

3.1.1. Effects of temperature

Temperature can have an effect on the reaction rate, as the Vant Hoff's law suggests that the reaction rate would be increased by 2–4 times with the increase of temperature by 10 K [31]. There is an exponential relationship between the reaction rate constant and temperature as described by the Arrhenius equation:

$$\ln K = -\frac{E_a}{RT} + \ln A \quad (10)$$

where K is the reaction rate constant, E_a is the activation energy, A is the pre-exponential factor, and R is the perfect gas constant.

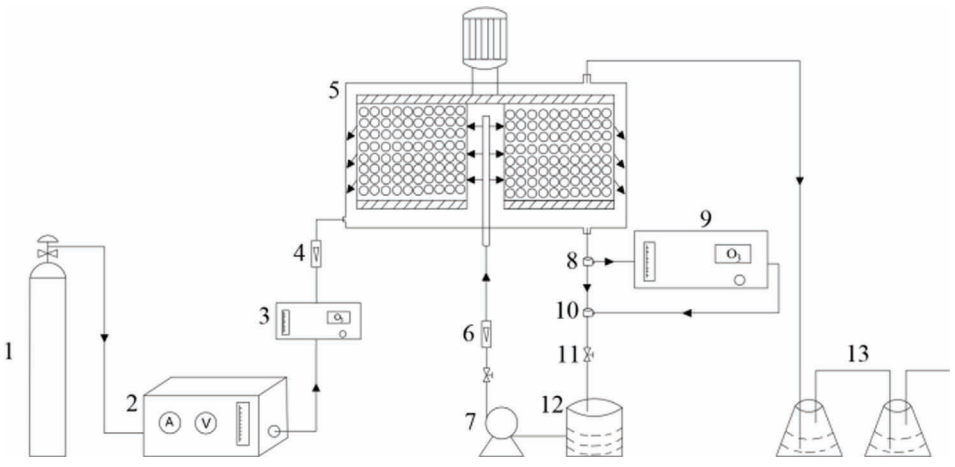

Fig. 1. Schematic of high-gravity intensified heterogeneous catalytic ozonation. 1-O_2 cylinder; 2-O_3 generator; 3-O_3 concentration detector; 4-gas flow meter; 5-RPB; 6-liquid flow meter; 7-circulating pump; 8, 10-tee; 9-liquid phase O_3 concentration detector; 11-valve; 12-storage tank; 13-exhaustgas treatment device.

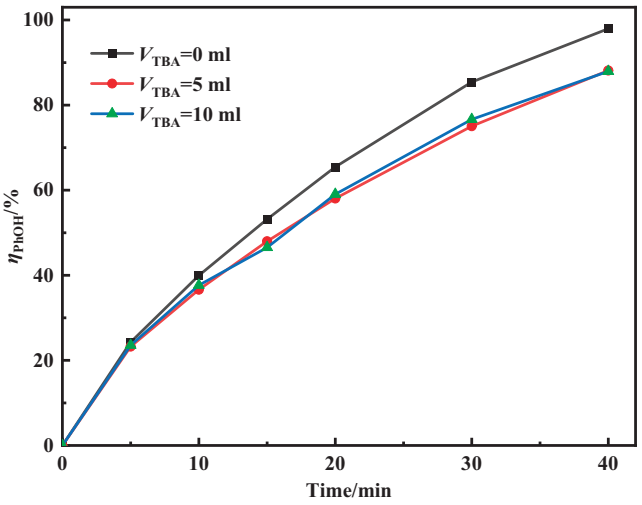

Fig. 2. The effect of TBA dosage on the removal rate of phenol (pH = 2, T = 293 K, β = 20, C_{O_3}=30 mg·L^{-1}, C_{PhOH}=100 mg·L^{-1}, Q_G = 60 L·h^{-1}, V_L = 80 L·h^{-1}).

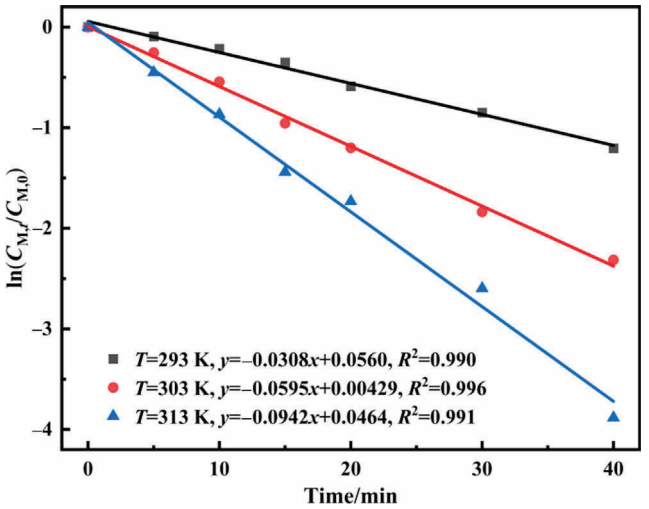

Fig. 4. The effect of temperature on the reaction rate of the direct reaction between O_3 and phenol in RPB (pH = 2, β = 20, C_{O_3}=30 mg·L^{-1}, C_{PhOH}=100 mg·L^{-1}, Q_G = 60 L·h^{-1}, V_L = 80 L·h^{-1}, V_{TBA} = 10 ml) T = 293, 303, 313 K, k_{app}=0.0308, 0.0595, 0.0942 min^{-1}.

It is known that temperature can affect the kinetics of direct reaction [32]. Specifically, as the temperatures rose, ozone becomes unstable because the activated molecules involved in the direct reaction are more likely to collide with each other to increase the reaction rate constant. In this experiment, the effect of temperature (293 K, 303 K, 313 K) on the direct reaction rate between O_3 and phenol is investigated, and the experimental results are shown in Fig. 4.

As shown in Fig. 4, the reaction rate is increased from 0.0308 min^{-1} at 293 K to 0.0595 min^{-1} at 303 K and then to 0.0942 min^{-1} at 313 K. In Arrhenius equation, the activation energy (E_a) can be regarded as a temperature independent constant. The pre-exponential factor (A) can be affected by the reaction rate constant and the collision frequency of molecules. Increasing the temperature will accelerate the collision frequency between ozone and phenol, which in turn promotes the reaction between ozone and phenol. However, it also noted that high temperature can adversely affect the mass transfer of O_3 [33,34]. In this study, it is found that the O_3 concentration in the liquid phase is close to 0, indicating that the direct reaction between O_3 and phenol is a fast reaction that occurs in liquid films [35]. Thus, change in O_3 solubility is unlikely to has an effect on the reaction rate. Overall, increasing the temperature can increase the reaction rate between O_3 and phenol [36].

3.1.2. Effect of initial solution pH

Fig. 5 reveals that the initial pH of the solution also has an effect on the reaction rate between O_3 and phenol. At 40 min, the reaction rate is 0.0421 min^{-1} at pH = 2, 0.0581 min^{-1} at pH = 4, 0.0920 min^{-1} at pH = 6, and 0.115 min^{-1} at pH = 8, respectively, which indicates that the direct reaction is increased at higher initial pH. The reason may be that the mass transfer rate of O_3 is increased with increasing initial pH [37], and thus O_3 will be decomposed at a higher rate and the equilibrium concentration will be reduced. Some dissolved O_3 can react directly with phenol, while the rest can be decomposed into ·OH under the effect of OH^- [38], which in turn can be completely captured by excess TBA. However, the O_3 concentration in the liquid phase is still close to 0 at high pH, confirming that the direct reaction between O_3 and phenol is a fast reaction.

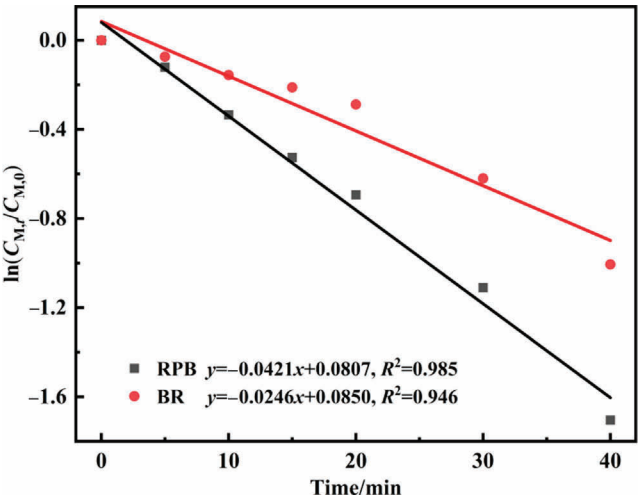

Fig. 3. The rate constant of the direct reaction between O_3 and phenol in RPB and BR (RPB: pH = 2, β = 20, C_{O_3}=30 mg·L^{-1}, C_{PhOH}=100 mg·L^{-1}, T = 293 K, V_{TBA} = 10 ml, Q_G = 60 L·h^{-1}, V_L = 80 L·h^{-1}; BR: pH = 2, T = 293 K, C_{O_3}=30 mg·L^{-1}, C_{PhOH}=100 mg·L^{-1}, V_{TBA} = 10 ml).

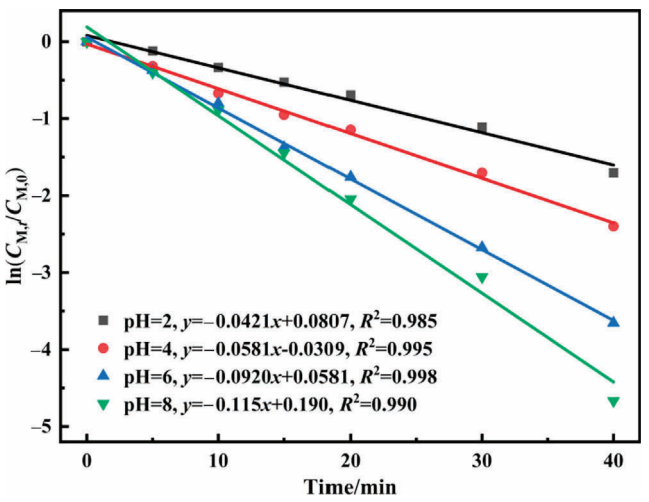

Fig. 5. The effect of the initial solution pH on the reaction rate between O_3 and phenol in RPB (β = 20, C_{O_3}=30 mg·L^{-1}, C_{PhOH}=100 mg·L^{-1}, T = 293 K, Q_G = 60 L·h^{-1}, V_L = 80 L·h^{-1}, V_{TBA} = 10 ml) pH = 2, 4, 6, 8, k_{app}=0.0421, 0.0581, 0.0920, 0.115 min^{-1}.

At pH = 6 which is close to the pH_{pzc} of Fe-Mn-CuO_X/γ-Al_2O_3 (6.24), M−OH is present on the catalyst surface with almost no charges, and the density and catalytic activity of hydroxyl groups reach the maximum [39]. Also, the dissolved O_3 can contact more frequently with the active sites on the catalyst surface, and thus more ·OH would be generated and then removed by excess TBA. The reaction equations between the hydroxyl groups on the catalyst surface and O_3 are shown in Eqs. (11) – (14). As the reaction rate between O_3 and phenol is much larger than that of the decomposition of O_3 adsorbed on the catalyst surface, pH has no obvious effect on the adsorption of O_3 on the catalyst surface. On the whole, increasing the solution pH increases the rate constant of the direct reaction between O_3 and phenol.

$$\equiv M - OH + O_3 \rightarrow \equiv M + \cdot O_2^- + \cdot HO_2 \quad (11)$$

$$\cdot O_2^- + O_3 \rightarrow \cdot O_3^- + O_2 \quad (12)$$

$$\cdot O_3^- + H^+ \rightarrow \cdot HO_3 \quad (13)$$

$$\cdot HO_3 \rightarrow \cdot OH + O_2 \quad (14)$$

3.1.3. Effect of high-gravity factor

The high-gravity factor (β) is a dimensionless parameter characterizing the intensity of the high-gravity field, and it is defined as the ratio of the centrifugal acceleration to the acceleration of gravity [40]:

$$\beta = \frac{G}{g} = \frac{r\omega^2}{g} = \frac{N^2 r}{894} \quad (15)$$

where r is the radius of the rotor, m; ω is the angular velocity of the rotor, s^{-1}; g is the acceleration of gravity, $m^2 \cdot s^{-1}$; N is the rotation speed of the rotor, $r \cdot min^{-1}$, which is controlled by adjusting the frequency converter. However, as the high-gravity factor is proportional to the square of the rotation speed of the rotor, the intensity of the high-gravity filed can be changed by adjusting the rotation speed of the rotor.

Fig. 6 reveals that at 40 min, the reaction rate is 0.0449 min^{-1} at β = 10, but it is increased to 0.0603 min^{-1} at β = 20 and then it is decreased to 0.0438 min^{-1} at β = 40. It is clear that the rotation speed is increased at higher high-gravity factors, and as a result the degree of liquid turbulence is increased and the liquid film becomes thinner, and the transfer of ozone from gas phase to liquid phase is promoted. The increase of β also allows the liquid to overcome the effect of surface tension and move in the catalysts at a very high speed and a very small scale [41]. However, the residence time of the liquid in the packing is inversely proportional to the high-gravity factor [42]. In this case, the reaction rate is reduced and more energy consumption and cost are required. Thus, the reaction rate between O_3 and phenol first increases and then decreases with the increase of high-gravity factor, and theoretically there should be an optimal high-gravity factor.

3.1.4. Effects of gas-phase O_3 concentration

Fig. 7 reveals that as the gas-phase O_3 concentration is increased from 10 $mg \cdot L^{-1}$ to 30 $mg \cdot L^{-1}$, the reaction rate is increased by 276% from 0.0160 min^{-1} to 0.0603 min^{-1}; while increasing the gas-phase O_3 concentration to 40 $mg \cdot L^{-1}$ results in a 44.1% increase in the reaction rate to 0.0869 min^{-1}. Obviously, increasing the gas-phase O_3 concentration can increase the driving force for the mass transfer of O_3 [43], and as a result phenol will be more likely to contact with O_3. However, at high gas-phase O_3 concentrations, more O_3 will be discharged before dissolution, leading to low utilization efficiency of O_3 [44] and consequently low reaction rate. Thus, an appropriate concentration of O_3 should be used in industrial applications.

3.2. Empirical kinetic model for high-gravity intensified heterogeneous catalytic ozonation

3.2.1. Plot of $lnk_{O_3,PhOH}$ against 1/T

The plot of $\ln k_{O_3,PhOH}$ against $1/T$ is shown in Fig. 8, where the correlation coefficient is R^2 = 0.991 and the slope is $k = -E_a/R$ = −2732.16. Then, the apparent activation energy of the direct reaction between O_3 and phenol is determined to be 16023.08 $J \cdot mol^{-1}$, and the pre-exponential factor A is 352.35.

3.2.2. Plot of $lnk_{O_3,PhOH}$ against lnC_{OH^-}

The plot of $\ln k_{O_3,PhOH}$ against $\ln C_{OH^-}$ is shown in Fig. 9, where the correlation coefficient is R^2 = 0.988 and the slope k is 0.0592.

3.2.3. Plot of $lnk_{O_3,PhOH}$ against $ln\ C_{O_3}$

The plot of $\ln k_{O_3,PhOH}$ against $\ln C_{O_3}$ is shown in Fig. 10, where the correlation coefficient is R^2 = 0.990 and the slope k is 1.23.

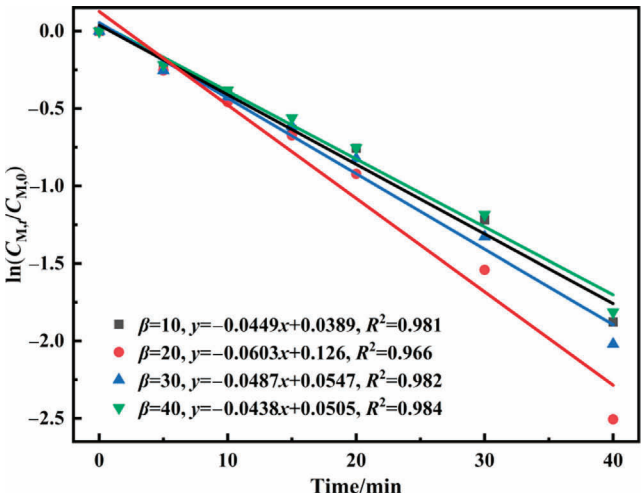

Fig. 6. The effect of high-gravity factor on the reaction rate of the direct reaction between O_3 and phenol in RPB (pH = 2, C_{O_3}=30 $mg \cdot L^{-1}$, C_{PhOH}=100 $mg \cdot L^{-1}$, T = 293 K, Q_G = 60 $L \cdot h^{-1}$, V_L = 80 $L \cdot h^{-1}$, V_{TBA} = 10 ml) β = 10, 20, 30, 40, k_{app}=0.0449, 0.0603, 0.0487, 0.0438 min^{-1}.

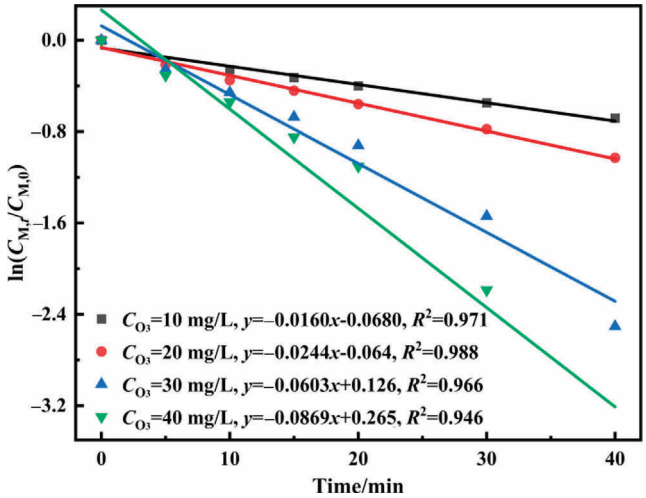

Fig. 7. The effect of gas-phase O_3 concentration on the reaction rate between O_3 and phenol in RPB (pH = 2, β = 20, C_{PhOH}=100 $mg \cdot L^{-1}$, T = 293 K, Q_G = 60 $L \cdot h^{-1}$, V_L = 80 $L \cdot h^{-1}$, V_{TBA} = 10 ml)C_{O_3} = 10, 20, 30, 40 $mg \cdot L^{-1}$, k_{app}=0.0160, 0.0244, 0.0603, 0.0869 min^{-1}.

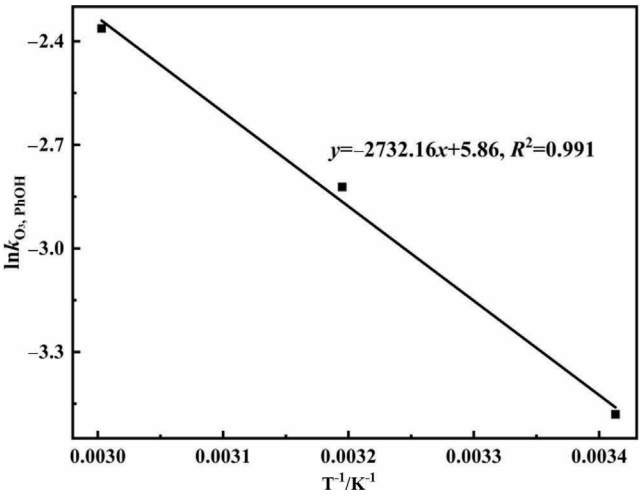

Fig. 8. The fitting curve of $\ln k_{O_3,PhOH}$ against $1/T$.

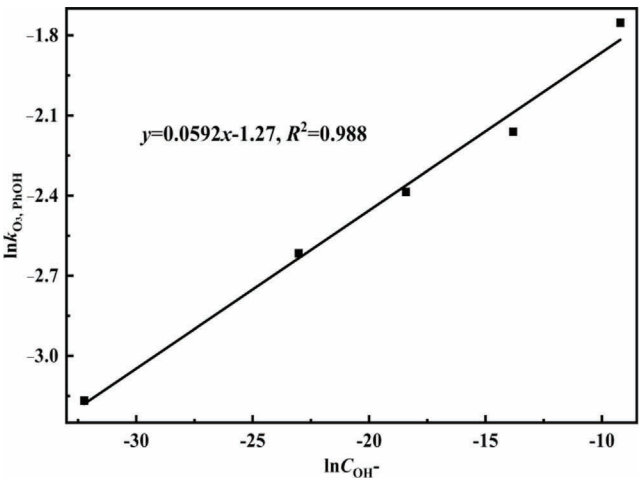

Fig. 9. The fitting curve of $\ln k_{O_3,PhOH}$ against $\ln C_{OH^-}$.

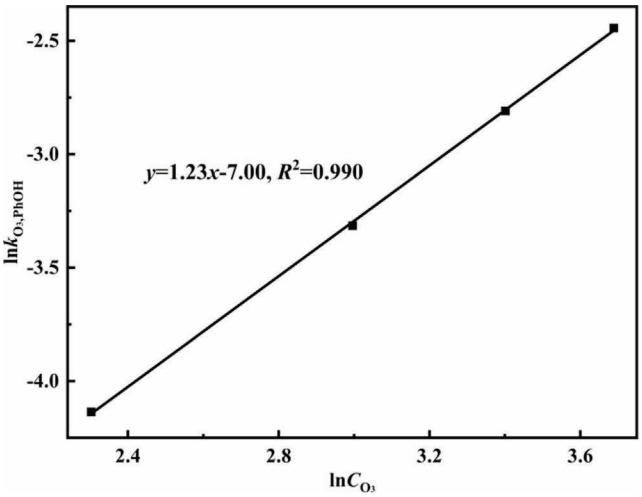

Fig. 10. The fitting curve of $\ln k_{O_3,PhOH}$ against $\ln C_{O_3}$.

3.2.4. Plot of $\ln k_{O_3,PhOH}$ against lnN

The plot of $\ln k_{O_3,PhOH}$ against ln$N$ is shown in Fig. 11, where the correlation coefficient is R^2 = 0.999 and the slope k = 0.326.

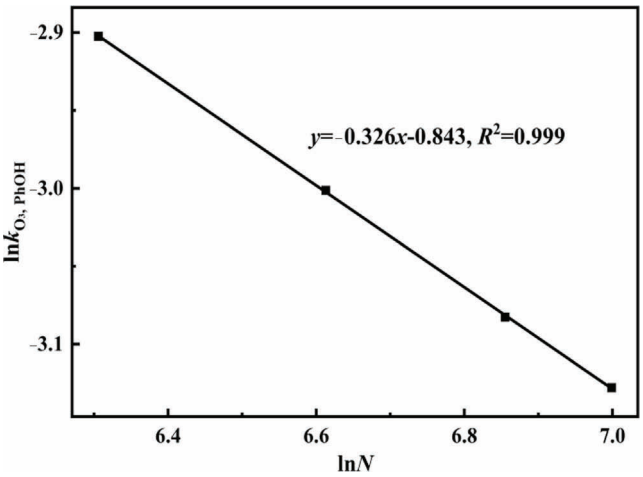

Fig. 11. The fitting curve of $\ln k_{O_3,PhOH}$ against ln$N$.

It follows from the linear regression equation that:

$$C_{PhOH,t} = C_{PhOH,0}\exp[352.35\exp(-16023.08/RT)]C_{OH^-}^{0.0592}C_{O_3}^{1.23}N^{0.326}t \quad (16)$$

It is seen that m, n and p are larger than 0, indicating that initial pH, gas-phase O_3 concentration and the rotation speed of the rotor are positively related to the rate constant. In addition, the E_a/R value is always larger than 0, indicating that the reaction rate increases with increasing temperature. According to the empirical kinetic model, the effects of these parameters on the degradation of phenol follow the order of gas-phase O_3 concentration C_{O_3} > the rotation speed of the rotor N > OH^- concentration C_{OH^-}.

4. Conclusions

In this study, excess TBA is used to eliminate the indirect reaction between phenol and ·OH generated from the decomposition of O_3, and the kinetics of the direct reaction between O_3 and phenol in RPB is investigated. It is revealed that in a high-gravity environment, the direct reaction between O_3 and phenol follows the pseudo-first-order kinetics with reaction rates in the range of 0.0160–0.115 min^{-1} under the conditions of T = 293–313 K, pH = 2–8, β = 10–40, and C_{O_3} = 10–40 $mg{\cdot}L^{-1}$. The O_3 concentration in the liquid phase is 0, indicating that the direct reaction between O_3 and phenol is a fast reaction that occurs on liquid films. The rate constant increases with the increase of temperature, initial solution pH and gas-phase O_3 concentration, but it increases and then decreases with the increase of high-gravity factor. Compared with BR, the direct reaction between O_3 and phenol is greatly intensified in RPB. An empirical power-exponential model is proposed for the high-gravity intensified heterogeneous catalytic ozonation of phenol, which reveals that temperature, initial solution pH, high-gravity factor, and gas-phase O_3 concentration have significant effects on the rate constant of the direct reaction between O_3 and phenol. Thus, it is concluded that the high-gravity technique can intensify the direct reaction between O_3 and phenol and thus enhance the degradation of phenol in wastewater.

Declaration of Competing Interest

The authors declare that they have no known competing financial interests or personal relationships that could have appeared to influence the work reported in this paper.

Acknowledgements

This work was supported by the Fund for Shanxi Province Higher Education "1331 Project" for Improving Quality and Efficiency Construction (nuc2021-006), Key Research & Development Plan of Shanxi Province (201903D321059), Scientific Activities of Selected Returned Overseas Professionals in Shanxi Province (20200004), Transformation and Cultivation Projects of Scientific and Technological Achievements in Universities of Shanxi Province Institutions (2020CG040).

References

[1] D.M. Naguib, N.M. Badawy, Phenol removal from wastewater using waste products, *J. Environ. Chem. Eng.* 8 (2019) 103592.
[2] S. Ahmed, M.G. Rasul, W.N. Martens, R. Brown, M.A. Hashib, Heterogeneous photocatalytic degradation of phenols in wastewater: A review on current status and developments, *Desalination* 261 (2010) 3–18.
[3] E. El-Ashtoukhy, Y.A. El-Taweel, O. Abdelwahab, E.M. Nassef, Treatment of petrochemical wastewater containing phenolic compounds by electrocoagulation using a fixed bed electrochemical reactor, *Int. J. Electrochem. Sci.* 8 (2013) 1534–1550.
[4] A.S. Fajardo, R.C. Martins, R.M. Quinta-Ferreira, Treatment of a simulated phenolic effluent by heterogeneous catalytic ozonation using Pt/Al_2O_3, *Environ. Technol.* 34 (2013) 301–311.
[5] Z.Q. Zeng, H.K. Zou, L. Xin, B.C. Sun, J.F. Chen, L. Shao, Ozonation of phenol with O_3/Fe (II) in acidic environment in a rotating packed bed, *Ind. Eng. Chem. Res.* 51 (2012) 10509–10516.
[6] H. Barndök, L. Cortijo, D. Hermosilla, C. Negro, Á. Blanco, Removal of 1,4-dioxane from industrial wastewaters: Routes of decomposition under different operational conditions to determine the ozone oxidation capacity, *J. Hazard. Mater.* 280 (2014) 340–347.
[7] T. Ueda, M. Hara, I. Odagawa, T. Shigihara, Simultaneous treatment of washing, disinfection and sterilization using ultrasonic levitation, silver electrolysis and ozone oxidation, *Biocontrol. Sci.* 14 (2009) 1.
[8] F.X. Deng, S. Qiu, C. Chen, X. Ding, F. Ma, Heterogeneous catalytic ozonation of refinery wastewater over alumina-supported Mn and Cu oxides catalyst, *Ozone: Sci. Eng.* 37 (2015) 546–555.
[9] S.J. Shao, D. Lei, Y. Song, L.N. Liang, Y.Z. Liu, W.Z. Jiao, Cu-MnO_X/gamma-Al_2O_3 catalyzed ozonation of nitrobenzene in a high-gravity rotating packed bed, *Ind. Eng. Chem. Res.* 60 (2021) 2123–2135.
[10] J. Valand, S. Maddila, H.B. Friedrich, S.B. Jonnalagadda, Heterogeneous catalyzed ozonation using Cu-Ni-Co oxides for degradation of dichlorophenol, *Ozone: Sci. Eng.* 38 (2016) 14–24.
[11] X.F. Li, W.Y. Chen, L.M. Ma, H.W. Wang, J.H. Fan, Industrial wastewater advanced treatment *via* catalytic ozonation with an Fe-based catalyst, *Chemosphere* 195 (2018) 336–343.
[12] H.D. Qin, Q.Z. Dong, H.L. Chen, G. Yang, X.M. Zhang, Kinetics and mechanism of humic acids degradation by ozone in the presence of CeO_2/AC, *Ozone: Sci. Eng.* 37 (2015) 371–378.
[13] L. Zhao, W.C. Ma, J. Ma, G. Wen, Q.L. Liu, Relationship between acceleration of hydroxyl radical initiation and increase of multiple-ultrasonic field amount in the process of ultrasound catalytic ozonation for degradation of nitrobenzene in aqueous solution, *Ultrason. Sonochem.* 22 (2015) 198–204.
[14] Y. Ku, Y.J. Huang, H.W. Chen, W.M. Hou, Decomposition of acetone by hydrogen peroxide/ozone process in a rotating packed contactor, *Water Environ. Res.* 83 (2011) 588–593.
[15] W.Z. Jiao, S. Luo, Z. He, Y.Z. Liu, Applications of high gravity technologies for wastewater treatment: A review, *Chem. Eng. J.* 313 (2017) 912–927.
[16] W.Z. Jiao, X.Y. Wei, S.J. Shao, Y.Z. Liu, Catalytic decomposition and mass transfer of aqueous ozone promoted by Fe-Mn-Cu/γ-Al_2O_3 in a rotating packed bed, *Chin. J. Chem. Eng.* 45 (2022) 133–142.
[17] D. Wang, T.R. Liu, L. Ma, F. Wang, L. Shao, Modeling and experimental studies on ozone absorption into phenolic solution in a rotating packed bed, *Ind. Eng. Chem. Res.* 58 (2019) 7052–7062.
[18] W.Z. Jiao, Y.J. Qin, Y.H. Wang, L. Guo, Y.Z. Liu, Enhancement performance of ozone mass transfer by high gravity technology, *Desalin. Water Treat.* 66 (2017) 195–202.
[19] X.Y. Wei, S.J. Shao, X. Ding, W.Z. Jiao, Y.Z. Liu, Degradation of phenol with heterogeneous catalytic ozonation enhanced by high gravity technology, *J. Cleaner Prod.* 248 (2020) 119179.
[20] Z.Q. Zeng, J.F. Wang, Z.H. Li, B.C. Sun, L. Shao, W.J. Li, J.F. Chen, H.K. Zou, The advanced oxidation process of phenol solution by O_3/H_2O_2 in a rotating packed bed, *Ozone: Sci. Eng.* 35 (2013) 101–108.
[21] Z.Q. Zeng, H.K. Zou, X. Li, M. Arowo, B.C. Sun, J.F. Chen, G.W. Chu, L. Shao, Degradation of phenol by ozone in the presence of Fenton reagent in a rotating packed bed, *Chem. Eng. J.* 229 (2013) 404–411.
[22] Y. Luo, G.W. Chu, H.K. Zou, Z.Q. Zhao, M. Dudukovic, Gas-liquid effective interfacial area in a rotating packed bed, *Ind. Eng. Chem. Res.* 51 (2012) 16320–16325.
[23] S.G. Zhang, Y.J. Qin, D.M. Zhang, W.Z. Jiao, L. Guo, Y.Z. Liu, Effects of coexisting substances on nitrobenzene degradation with O_3/H_2O_2 process in high-gravity fields, *China Pet. Process. Petrochem. Technol.* 18 (2016) 32–40.
[24] G. Teixeira, A. Cruz, G. Samanamud, A. França, L. Naves, D. Melo, D. Morais, E. Baston, F. Naves, The use of nanovermiculite catalyst in the study of removal of the organic load and degradation of atrazine via ozone process in RPB reactor, *J. Environ. Sci. Health, Part B* 55 (2020) 19–29.
[25] W.Z. Jiao, P.Z. Yang, W.Q. Gao, J.J. Qiao, Y.Z. Liu, Apparent kinetics of the ozone oxidation of nitrobenzene in aqueous solution enhanced by high gravity technology, *Chem. Eng. Process.* 146 (2019) 107690.
[26] B. Philip, Errata-the reaction of ozone with organic compounds, *Chem. Rev.* 59 (1959) 179–180.
[27] J. Hoigné, H. Bader, Rate constants of reactions of ozone with organic and inorganic compounds in water-I: Non-dissociating organic compounds, *Water. Res.* 17 (1983) 173–183.
[28] J. Hoigné, H. Bader, Rate constants of reactions of ozone with organic and inorganic compounds in water-II: inorganic compounds and radicals, *Water. Res.* 19 (1985) 993–1004.
[29] P.Z. Yang, S. Luo, H.Y. Liu, W.Z. Jiao, Y.Z. Liu, Aqueous ozone decomposition kinetics in a rotating packed bed, *J. Taiwan. Inst. Chem. Eng.* 96 (2019) 11–17.
[30] F.J. Beltrán, J.F. García-Araya, B. Acedo, Advanced oxidation of atrazine in water-I. Ozonation, *Water Res.* 28 (1994) 2153–2164.
[31] P.J. Skrdla, V. Antonucci, C. Lindemann, Tautomer interconversion of 2,4-pentanedione during gas chromatography on an oxidized cyano-modified capillary column, *J. Chromatogr. Sci.* 39 (2001) 431–440.
[32] M.D. Gurol, P.C. Singer, Kinetics of ozone decomposition: A dynamic approach, *Environ. Sci. Technol.* 16 (1982) 377–383.
[33] L. Zhao, J. Ma, Z.Z. Sun, H.L. Liu, Mechanism of heterogeneous catalytic ozonation of nitro-benzene in aqueous solution with modified ceramic honeycomb, *Appl. Catal, B.* 89 (2009) 326–334.
[34] Y. Jung, E. Hong, M. Kwon, J.W. Kang, A kinetic study of ozone decay and bromine formation in saltwater ozonation: Effect of O_3 dosage, salinity, pH, and temperature, *Chem. Eng. J.* 312 (2017) 30–38.
[35] C.C. Chang, C.Y. Chiu, C.Y. Chang, C.F. Chang, Y.H. Chen, D.R. Ji, J.Y. Tseng, Y.H. Yu, Pt-catalyzed ozonation of aqueous phenol solution using high-gravity rotating packed bed, *J. Hazard. Mater.* 168 (2009) 649–655.
[36] M.G. El-Din, D.W. Smith, F.A. Momani, W.X. Wang, Oxidation of resin and fatty acids by ozone: Kinetics and toxicity study, *Water. Res.* 40 (2006) 392–400.
[37] F.J. Beltrán, Ozone reaction kinetics for water and wastewater system, CRC Press, Florida, 2004.
[38] C.C. Lin, C.Y. Chao, M.Y. Liu, Removal of ozone from air by absorption in a rotating packed bed, *J. Ind. Eng. Chem.* 16 (2010) 140–146.
[39] S.J. Shao, W.Z. Jiao, Y.Z. Liu, Research progress of high gravity enhanced ozone-based advanced oxidation technology, *Chem. Ind. Eng. Prog.* 39 (2020) 4798–4811.
[40] Y. Liu, Y. Luo, G.W. Chu, F. Larachi, H.K. Zou, J.F. Chen, Liquid microflow inside the packing of a rotating packed bed reactor: Computational, observational and experimental studies, *Chem. Eng. J.* 386 (2020) 121134.
[41] W.Z. Jiao, Y.Z. Liu, W.L. Liu, J. Li, F. Shao, C.R. Wang, Degradation of wastewater containing nitrobenzene with O_3 and H_2O_2 by high gravity technology, *China Pet. Process. Petrochem. Technol.* 15 (2013) 85–94.
[42] C.C. Lin, B.C. Chen, Y.S. Chen, S.K. Hsu, Feasibility of a cross-flow rotating packed bed in removing carbon dioxide from gaseous streams, *Sep. Purif. Technol.* 62 (2008) 507–512.
[43] A. Aghaeinejad-Meybodi, A. Ebadi, S. Shafiei, A. Khataeec, A.D. Kiadehid, Degradation of fluoxetine using catalytic ozonation in aqueous media in the presence of nano-γ-alumina catalyst: Experimental, modeling and optimization study, *Sep. Purif. Technol.* 211 (2019) 551–563.
[44] J. Wang, X. Quan, S. Chen, H.T. Yu, G.B. Liu, Enhanced catalytic ozonation by highly dispersed CeO_2 on carbon nanotubes for mineralization of organic pollutants, *J. Hazard. Mater.* 368 (2019) 621–629.